Matching Flexible Polygons to Fields of Corners Extracted from Images[1]

Siddharth Manay and David W. Paglieroni

Lawrence Livermore National Laboratory
7000 East Ave, Livermore, CA 94551, USA

Abstract. We propose a novel efficient method that finds partial and complete matches to models for families of polygons in fields of corners extracted from images. The polygon models assign specific values of acuteness to each corner in a fixed-length sequence along the boundary. The absolute and relative lengths of sides can be either constrained or left unconstrained by the model. Candidate matches are found by using the model as a guide in linking corners previously extracted from images. Geometrical similarity is computed by comparing corner acutenesses and side lengths for candidate polygons to the model. Photometric similarity is derived by comparing directions of sides in candidate polygons to pixel gradient directions in the image. The flexibility and efficiency of our method is demonstrated by searching for families of buildings in large overhead images.

Keywords. Corner Extraction, Polygon Extraction, Overhead Imagery

1. Introduction

Broad area image search involves detecting localized objects (vehicles, buildings, storage tanks, parking lots, etc.) in overhead images with broad area coverage. Many objects of interest can be at least partially modeled as polygons (e.g., roofs of buildings or vehicles). In this paper, we propose a class of polygon models invariant to position / orientation and, if desired, also invariant to scale or even some shape distortions. We then construct similarity measures based on geometric and photometric considerations for computing the degree of match between objects in images and the polygon model.

Our general idea is to extract corners from images using a robust technique previously developed in [1-2]. We then develop a highly efficient matching strategy that grows all possible polygon trees of corners from the field of corners detected in the image, and seeks tree branches corresponding to successful complete or partial matches to the polygon model. The matches are validated and redundancies are eliminated.

Polygon matching methods based on polygon trees of corners provide several advantages: (1) They are highly efficient. (2) They are robust to photometric variation in the image, such as lighting changes and object contrast. (3) They are invariant to polygon position / orientation, and, if desired, they can also be made invariant to

[1] Work performed under the auspices of the U.S. Department of Energy by the University of California, Lawrence Livermore National Laboratory under Contract No. W-7405-Eng-48 (UCRL-CONF-226354).

polygon scale or relative side lengths. (4) They are relatively insensitive to broken edges because they are not based on edge detection. (5) They can handle missing or occluded corners.

Section 2 discusses our proposed method in the context of prior work on polygon detection. Section 3 reviews a previously developed corner detection algorithm that matches models of corners to gradient directions in the image. A very simple yet flexible way to model polygons is developed in Section 4. Geometric and photometric measures of similarity between polygon matches and polygon models are developed in Section 5. An efficient algorithm for growing polygon trees from fields of corners previously extracted from images is developed in Section 6. A method for eliminating redundant polygon matches is developed in Section 7. Then in Section 8, our approach is applied to the problem of finding buildings of certain general shapes in large overhead images.

2. Prior Work

Due to the polygonal nature of many objects constructed by humans that appear in images, polygon and rectangle detection are important topics of research. Although a complete literature survey is beyond the scope of this paper, selected key research is briefly reviewed below.

The search for polygonal objects in images is often performed in two stages: (1) search for primitive features, such as edges, lines, or corners, and (2) assembling collections of these features into polygons. Under specific assumptions about the desired shape (e.g. rectangles) features can be grouped by a variety of algorithms and constraints [3-9]. More generally, features can be linked into chains, trees, or graphs, which are then searched for matches to polygons [10-13]. Although the preferred features are edges or lines extracted with edge detectors or Hough methods, corner detectors were employed directly in [10]. Higher-dimensional Hough methods transform edges directly into parameterized rectangles and regular polygons [14-15]. Other methods that estimate parameters directly include genetic algorithms [16] and algorithms that estimate posterior probability in the parameter space [17]. Due to their reliance on parameterization, these methods do not extend well to general polygons. Alternatively, over-segmented regions can be grouped into polygonal regions [18-19].

Rather than using extracted features, the image can be searched directly for template matches to the desired shape [20-21]. Templates allow little flexibility in the scale or shape of the object. Invariant models are employed to provide such flexibility. Polygon models composed of ordered lists of attributes (such as interior angles) can be applied to prune or validate feature graphs [13], fit to features directly using least-squares [22] or fit to images directly using iterative optimization [23-24]. Other instances of invariant models include polygons with side normal vectors fit to image gradients via eigenanalysis [25], contour models fit to an over-segmentation [l9], and triangulated models fit to image data with an inductive, brute force algorithm [26]. These models allow affine shape distortions (e.g., in [26], the shapes are triangles).

Like the attribute list models cited above, the polygonal model proposed in Section 4 is a special simplified case of invariant shape representations proposed by other authors (e.g., [27-29]), and shares many of their desirable properties, such as

invariance to rotation, translation, scale, and other shape distortions. However, we do not use optimization techniques to search for polygons, as these can be slow, require good initialization, and frequently find local minima for the objective functions. Instead, we adopt a philosophy published in much of the rectangle and polygon literature in which polygons are assembled from lower level components detected in images [3,6]. However, we choose lower level components based on corners rather than edges, and are thus less subject to problems associated with missing or broken edges. This approach requires a robust method for corner detection, such as the method based on gradient direction matching reviewed in the next Section. The ability to detect and analyze incomplete or partial polygons provides additional robustness to missing corners, which frequently occur due to occlusion, poor image quality, etc. Other corner detectors, such as those in [30-31], compute only the corner location, and not the orientation and acuteness attributes required to efficiently construct polygon trees.

In further contrast to methods in the literature, the proposed method leverages constraints in corner models and flexible polygon models to efficiently link corners into well-pruned polygon trees, and proposes a similarity measure for polygons, based on geometric and photometric factors, that captures the confidence in the detected polygon.

3. Modeling and Detecting Corners

As illustrated in Fig.1, models of corners have several attributes: corner [column, row] pixel location [c, r], corner acuteness $\alpha \in (0,\pi)$, corner orientation θ, corner leg length L and corner leg thickness T.

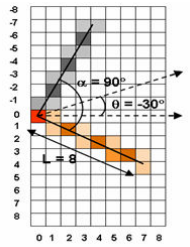

Fig.1 Model of a corner.

We use *gradient direction matching* (*GDM*) to detect corners in images [1,2]. Conceptually, a corner model is matched at all pixels and across a number of orientations to a field of pixel gradient directions using the GDM measure

$$S(\Delta_c,\Delta_r) = \sum_{(c,r)\in C} w(c,r)\cos^2[\theta(c+\Delta_c,r+\Delta_r) - \beta(c,r)] \qquad (1)$$

In equation (1), $\theta(c,r)$ is the image gradient direction at pixel (c,r), C is the set of all pixels on legs in the corner model (excluding the vertex itself, where normals are ambiguous), $\beta(c,r)$ is the angle normal to the leg containing pixel (c,r), and $w(c,r)$ is the weight assigned to leg pixel (c,r). $S \in [0,1]$ (1 for perfect matches) because the weights $w(c,r)$ are non-negative and sum to one. $w(c,r)$ decreases as the distance from the center of pixel (c,r) to the line segment representing its ideal leg increases. An

efficient FFT-based algorithm for computing the best match across all corner orientations at each pixel is given in [1]. As shown in Fig. 2, corners map to unambiguous local maxima in the degree of match. Because GDM relies on a sum of gradient angle (and not gradient magnitude) terms, it is robust to noise; see [2] for an extended discussion.

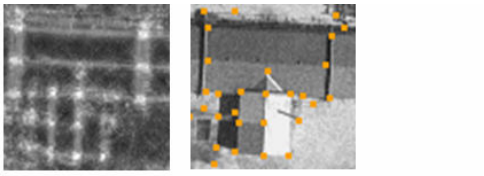

Fig.2 Corner detection example: (a) Optimal 90° corner match vs. location in an image. (b) Unambiguous local maxima.

4. Polygon Models

A polygon with n corners can be modeled as a sequence of parameter vectors for corners and side lengths in order of clockwise traversal along the boundary:

$$P^* = \{ [\alpha^*(k), L^*(k)] \quad k = 0...n-1 \} \tag{2}$$

$\alpha^*(k) \in (0,2\pi)$ (exclusive of π) is the acuteness of polygon corner k. $L^*(k) \geq 0$ is a length parameter for side k, which connects corner k to corner $((k+1) \bmod n)$. $\alpha^*(k) < \pi$ for convex corners and $\alpha^*(k) > \pi$ for concave corners. The relative orientation from corner k to corner $((k+1) \bmod n)$ can be computed directly from the corner acutenesses as

$$\begin{aligned} \Delta_\theta^*(k) &\stackrel{\Delta}{=} \theta^*((k+1) \bmod n) - \theta^*(k) \\ &= \pi - \frac{\alpha^*((k+1) \bmod n) + \alpha^*(k)}{2} \end{aligned} \tag{3}$$

where $\theta^*(k) \in [0,2\pi)$ is the absolute orientation of corner k. Note that $\theta^*(k)$ is *not* part of the model.

If side absolute lengths are to be specified (the goal is to find polygons of specific shape and size at any position or rotation), then for $k = 0...n-1$, specify $L^*(k) > 0$ as the prescribed length for side k. If only side relative lengths are to be specified (the goal is to find polygons of specific shape but any size), then set $L^*(0) = 0$ (undefined) and for $k = 1...n-1$, specify $L^*(k) > 0$ as the prescribed ratio of side k length to side 0 length. If side lengths are to be unconstrained, then for $k = 0...n-1$, set $L^*(k) = 0$ (undefined). Note that the model in equation (2) is always invariant to polygon position and rotation, whether or not the side lengths are constrained.

5. Polygon Similarity Measures

Let P be a candidate match to polygon model P^* (equation (2)) found by linking corners previously extracted from an image (Section 3). A method for using the model as a guide in linking corners previously extracted from images will be given in Section 6. In this Section, measures of similarity between P and P^* based on geometric and

photometric considerations are developed.

P can be either a complete or partial match to P^*. Although the similarity measures defined below allow complete and partial matches to be ranked together, they can harshly penalize partial matches relative to complete matches. As an alternative, one may therefore instead choose to rank matches with $n' \leq n$ corners only against other matches with exactly n' corners. The similarity measures defined below apply independent of n'.

First, geometric measures of similarity based on corner acuteness and relative or absolute side length are proposed. *Acuteness similarity* can be defined as

$$S_{\alpha}(P;P^*) = 1 - \frac{1}{2\pi n} \sum_{k=0}^{n-1} | \alpha(k) - \alpha^*(k) | \in [0,1] \qquad (4)$$

where $\alpha(k)$ is computed from the locations of corners k, $((k-1) \bmod n)$, and $((k+1) \bmod n)$ in P. If corner k is missing from P, set $|\alpha(k) - \alpha^*(k)| = 2\pi$ in equation (4).

Side length similarity can be defined as

$$S_L(P;P^*) = 1 - \frac{\sum_{k=0}^{n-1} |L(k) - L^*(k)|}{\sum_{k=0}^{n-1} L^*(k)} \in [0,1] \qquad (5)$$

when the side lengths are constrained (set $S_L(P;P^*) = 1$ when the side lengths are unconstrained). When side lengths are relative, $L(k)$ is the ratio of side k to side 0. If side k is missing from P, use $L(k) = 0$ in equation (5).

A photometric measure of similarity between polygons based on gradient direction matching (GDM) is proposed. This *gradient direction similarity* measure is similar to the measure used for detecting corners in equation (1), except it is tailored to polygons:

$$S_G(P;P^*) = \frac{1}{L} \sum_{(c,r) \in P} cos^2[\theta(c,r) - \beta(c,r)] \in [0,1] \qquad (6)$$

P can either be a complete or incomplete polygon match. However, the sum in equation (6) excludes polygon vertices, since normals are ambiguous there. Following equation (1), $\theta(c,r)$ is the image gradient direction at pixel (c,r), $\beta(c,r)$ is the angle normal to the side of P containing pixel (c,r), and L is the perimeter of the polygon match extrapolated to completeness.

The overall similarity between P and P^* combines the geometric and photometric similarities in equations (4)-(6):

$$S(P;P^*) = [w_{\alpha} \cdot S_{\alpha}(P;P^*)] * [w_L \cdot S_L(P;P^*)] * [w_G \cdot S_G(P;P^*)] \qquad (7)$$

where the weights are non-negative and specified such that $S(P;P^*) \in [0,1]$. "*" is some operator, such as "scalar sum", "scalar product", or "logical AND". For "logical AND" the weights are all 1 and the S values are set to 1 if greater than a threshold (0 otherwise). For match validation, we use "logical AND". For match comparison, we use $w_{\alpha} = 0$, $w_L = 0$, and $w_G = 1$, and "scalar sum" (in which case, $S(P;P^*) = S_G(P;P^*)$).

6. Polygon Trees

A *polygon tree* is a tree whose nodes represent corners in polygon matches P to a polygon model P^*, and whose branches represent connections between successive corners traversed in order along the boundary of P. As illustrated in Fig.3, each polygon tree has a single root node representing the corner from which traversal begins. A *branch* is a path from root to leaf. For polygon models with n corners, *complete branches* traverse n nodes, and *partial branches* traverse at least 2 nodes but less than n nodes.

Valid branches can be extrapolated to valid complete polygon matches. Whether complete or partial, branches are always valid when side lengths are constrained by the polygon model in either a relative or absolute sense. Identifying invalid partial branches for a model with unconstrained side lengths is of lesser importance but a topic of future research. Valid partial branches correspond to partial matches, and valid complete branches correspond to complete matches.

In Fig.3, branches ABCD and AJKL are complete and successful because corners D and L can be connected back to corner A in accordance with the polygon model constraints. Branch ABCE is complete but unsuccessful because E cannot be connected back to A. Branch AGH is partial and successful because H can be connected back to A through a missing corner H′. Branches AF and AGI are partial and unsuccessful because F and I cannot be connected back to A. In summary, ABCD and AJKL represent sequences of corners for a complete match, and AGH represents a sequence of corners for a partial match. A similarity to the model can be computed for each of these three matches using equation (7).

A partial branch is said to be finished if it is as complete as possible. Thus, for *finished partial branches*, given matches to corner 0 and corner 1 of the polygon model, there is no match to corner $n-1$. All polygon matches of interest correspond either to valid complete branches or valid finished partial branches.

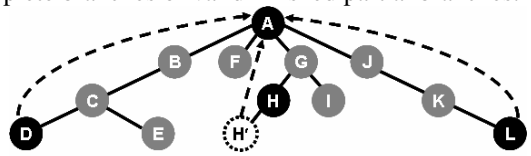

Fig.3 Polygon tree for a quadrilateral.

6.1. Tests for Candidate Corners

Let Ω be a field of corners with various positions, orientations, and acutenesses extracted from an image. Suppose $\boldsymbol{v}_k = [c_k, r_k, \alpha_k, \theta_k] \in \Omega$ was previously identified as a candidate for corner k in a match P to some polygon model P^*. Consider another corner $\boldsymbol{v} = [c, r, \alpha, \theta] \in \Omega$. We wish to devise tests based on corner acuteness, orientation, and location for determining whether or not $\boldsymbol{v}$ constitutes a candidate for corner $k+1 \in [1,n)$ in a polygon match to P^*.

First, $\boldsymbol{v}$ cannot be a candidate unless it satisfies the acuteness test

$$\alpha \in [\, \alpha^*(k+1) - \varepsilon_\alpha,\ \alpha^*(k+1) + \varepsilon_\alpha \,] \tag{8}$$

and the orientation test

$$\theta - \theta_k \in [\, \Delta_\theta^*(k) - \varepsilon_\theta,\ \Delta_\theta^*(k) + \varepsilon_\theta \,] \tag{9}$$

where $\Delta_\theta^*(k)$ is given by equation (3).

If P^* has absolute side length constraints, or P^* has relative side length constraints and $k > 0$, then the length of side k in the polygon match is expected to be

$$d_k = \begin{cases} L^*(k) & \text{for absolute constraints} \\ d_0 \cdot L^*(k) & \text{for relative constraints} \end{cases} \tag{10}$$

The angle of the ray emanating from $\boldsymbol{v}_k$ along side k is expected to be

$$\phi_k = \theta_k^+ \triangleq \theta_k + \alpha_k / 2 \ \text{ or } \ \theta_k^- \triangleq \theta_k - \alpha_k / 2 \tag{11}$$

Use $\phi_k = \theta_k^+$ if $[c_{k-1}, r_{k-1}]$ is closer to the line from $[c_k, r_k]$ in direction θ_k^- than from the line in direction θ_k^+. Otherwise, use $\phi_k = \theta_k^-$. $\boldsymbol{v}$ is expected to be at location

$$[c_{k+1}, r_{k+1}] = [c_k + d_k \cos\phi_k,\ r_k + d_k \sin\phi_k] \tag{12}$$

In this case, $\boldsymbol{v}$ is a candidate for corner $k+1$ if it satisfies the location test

$$\| [c - c_{k+1},\ r - r_{k+1}] \| \le \varepsilon_R \tag{13}$$

If P^* has no side length constraints, or P^* has relative side length constraints and $k = 0$, then the distance D from $[c, r]$ to the line $\mathcal{L}_k$ emanating from $[c_k, r_k]$ in direction ϕ_k must be small:

$$D(\, [c, r], \mathcal{L}_k \,) \le \varepsilon_R \tag{14}$$

For purposes of this paper, the angular and radial tolerances ε_θ, ε_α, and ε_R are treated as user-specified.

For $k = n-1$, it is necessary to determine whether or not $\boldsymbol{v}_0$ (the root corner in the polygon tree drawn from Ω) satisfies the conditions outlined in equations (8)-(14). A complete polygon match has been found only if it does.

6.2. Growing Polygon Trees

Let us now consider the problem of extracting all complete and partial polygon matches to a polygon model P^* from a field Ω of corners extracted from an image. Every corner in Ω with acuteness equal to $\alpha^*(0)$ is an eligible polygon tree root. An attempt is made to grow a polygon tree from each eligible root. Each grown tree may contain multiple complete and partial polygon matches.

For each eligible root, a polygon tree is grown by finding all corners that connect to the root corner using the tests given in Section 6.1. For each leaf, the process is repeated. The tree is grown in this way until it has n levels or cannot be grown further.

This process finds all complete matches. However, if all model corners do not have the same acuteness, the only way to guarantee that all finished partial matches will be found is to grow polygon trees as matches to every circular shift of the sequence of

model corners. In the end, each valid complete branch and each valid finished partial branch is catalogued for each polygon tree.

If each corner in a polygon tree can be linked to on average k candidate corners, each n-level polygon tree will have on average k^n branches. Values of n are typically between 4 (for a rectangle) and 10. The field of corners Ω contains n_Ω corners, where n_Ω is typically between 1000-8000. A very naïve attempt to grow polygon trees by assuming each corner may link to any other corner would result in n_Ω^n branches for each root corner and an $O(n_\Omega^{n+1})$ extraction algorithm. However, by leveraging corner models that include acuteness and orientation, polygon models, and the tests in Section 6.1 to restrict the search, k is reduced to a value much smaller than n_Ω. The result is an $O(n_\Omega k^n)$ extraction algorithm.

7. Match Validation and Redundancy

Polygon matches for which acuteness similarity $S_\alpha(P;P^*)$, side length similarity $S_L(P;P^*)$, or gradient direction similarity $S_G(P;P^*)$ are smaller than their respective user-specified similarity thresholds can be discarded. Additional matches can be discarded by applying user-specified size-dependent constraints on area, perimeter, minimum numbers of corners in partial matches, or ranges of admissible side lengths.

The surviving matches are ranked. However, some may be redundant in the sense that they overlap or are too close together. The idea behind match disambiguation is that in a set of overlapping polygon matches, only the match P of greatest similarity $S(P;P^*) = S_G(P;P^*)$ to P^* survives.

The distance between two polygons can be estimated using the symmetric (two-sided) Hausdorff distance D between two polygon matches P_1 and P_2 with n_1 and n_2 corners respectively:

$$D(P_1,P_2) = min\,[\, D_{ASYM}(P_1,P_2), D_{ASYM}(P_2,P_1)\,] \quad (15)$$

$$D_{ASYM}(P_1,P_2) = \max_{i=0\ldots n_1-1} \left(\min_{j=0\ldots n_2-1} \| [c_1(i) - c_2(j), r_1(i) - r_2(j)] \| \right) \quad (16)$$

where D_{ASYM} is the asymmetric (one-sided) Hausdorff distance [32]. Two polygon matches are said to be redundant if the symmetric Hausdorff distance between their corners is less than some threshold. For efficiency, polygons are spatially indexed, and for each polygon, the distance is computed only to polygons that likely overlap.

8. Experimental Results

Results of a polygon search experiment involving a large overhead satellite image are presented in this Section. Fig.4 shows an 4096 x 4096 pixel section of a satellite

image of Stockton, CA (courtesy of CASIL [33]). We searched for L-shaped buildings. Ranked results for three searches are shown: one for no side length constraints in Fig.5, one for relative side length constraints in Fig.6, and one for absolute side length constraints in Fig.7. Six sided polygon models for these three cases are given in Table 1.

Table 1: Specifications for L-Shaped Building Models

Model	Parameters
No side length	$\alpha^* = \{3\pi/2, \pi/2, \pi/2, \pi/2, \pi/2, \pi/2\}$
Relative side length	$\alpha^* = \{3\pi/2, \pi/2, \pi/2, \pi/2, \pi/2, \pi/2\}$, $L^* = \{60, 30, 90, 45, 30, 15\}$
Absolute side length	$\alpha^* = \{3\pi/2, \pi/2, \pi/2, \pi/2, \pi/2, \pi/2\}$, $L^* = \{4, 2, 6, 3, 2, 1\}$

As shown in Fig.5, polygon trees constrained by the model with no side length constraints detect L-shaped polygons of several sizes and proportions. For this experiment, partial polygons with less than four corners were discarded, while polygons with five corners are completed by extrapolating to compute the sixth vertex. The highest-ranked thumbnails are subjectively good fits to either discrete L-shaped buildings or sets of buildings in an L-shaped arrangement. There were some missed detections, and these are primarily attributed to inaccurate corners, missing corners (due to poor contrast or occlusion), or poor pixel gradient correlations (due to poor contrast, noise, or scene clutter).

In Fig. 6-7, absolute and relative side length constraints were imposed by the model to find L-shaped buildings with specific dimensions (reflected by the first thumbnail in each figure). In these cases, successful partial matches with as few as four corners were allowed.

Fig. 4 4096 x 4096 satellite image.

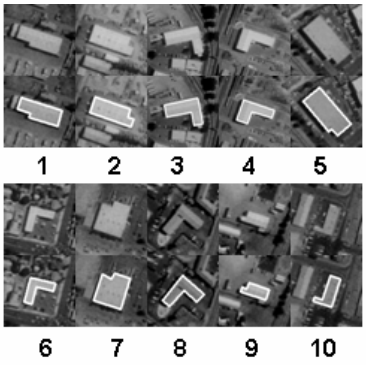

Fig. 5 Thumbnails of top 10 matches to L-shaped model with no side length constraints.

Fig. 6 Thumbnails of top 5 matches to L-shaped model with relative side length constraints.

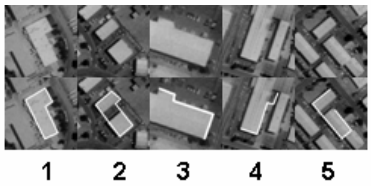

Fig.7. Thumbnails of top 5 matches to L-shaped model with absolute side length constraints.

Table 2 contains execution times for the above experiments. Note that the corners are pre-computed, so the corner extraction time is reported separately. For processing, the image is divided into 1024 x 1024 pixel image blocks. Reported times are the average time for the image blocks. All experiments were performed on a single core of an Intel Xeon 2.66GHz processor. The table demonstrates the relationship between the number of constraints in the model and the execution time of the algorithm.

Table 2: Algorithm Execution Time

Algorithm	Avg. Time per Image Block
Corner Extraction	47.4s
Polygon Extraction w/ no side length model	8.8s
Polygon Extraction w/ Relative side length model	1.9s
Polygon Extraction w/ Absolute side length model	0.7s

9. Conclusion

A novel efficient method that matches models for families of polygons to fields of corners extracted from images has been developed. The flexibility of our method was demonstrated by searching for buildings of prescribed shape in large overhead images, subject to various degrees of constraint on lengths of the polygon sides.

The method requires all possible polygon trees to be grown from the field of corners, subject to model constraints. Each tree can contain several valid complete and partial matches. However, the similarity measures for polygons in equations (4)-(6) harshly penalize partial matches relative to complete matches, thus making it problematic to rank partial and complete matches together. We thus plan to extend our work by using gradient direction matches for corners and sides as random state variables in Hidden Markov Model representations for polygon matches so that complete and partial matches can be ranked together in a more even-handed statistically rigorous way.

References

1. Paglieroni, D., Eppler, W., Poland, D.: Phase sensitive cuing for 3D objects in overhead images. In: SPIE Defense and Security Symposium: Signal Processing, Sensor Fusion and Target Recognition XIV, Proc. SPIE. Volume 5809. (Mar. 2005) 28–30
2. Paglieroni, D., Manay, S.: Signal-to-noise behavior of corners modeled as image gradient direction fields. In: Defense and Security Symposium, Proc. SPIE. (Apr. 2007)
3. Kim, H., Choi, W., Kim, H.: A hierarchical approach to extracting polygons based on perceptual grouping. In: Sys.Man, and Cybernetics, IEEE Int'l Conf. on. Volume 3. (Oct. 1994) 2402–2407
4. Lin, C., Nevatia, R.: Building detection and description from a single intensity image. Comp. Vis and Image Understanding 72(2) (1998) 101–121
5. Lagunovsky, D., Ablameyko, S.: Straight-line-based primitive extraction in gray-scale object recognition. Pat. Rec. Let. 20(10) (Oct. 1999) 1005–1014
6. Tao, W., Tian, J., Liu, J.: A new approach to extract rectangular buildings from aerial urban images. In: Sig. Proc., Int'l Conf. on. Volume 1. (Aug. 2002) 143–146
7. Yu, Z., Bajaj, C.: Detecting circular and rectangular particles based on geometric feature detection in electron micrographs. J. Structural Biology 145 (2004) 168–180
8. Liu, D., He, L., Carin, L.: Airport detection in large aerial optical imagery. In: Acoustics, Speech, and Signal Proc. IEEE Int'l Conf. on. Volume 5. (May 2004)
9. Liu, Y., Ikenaga, T., Goto, S.: Geometrical physical and text/symbol analysis based approach of traffic sign detection system. In: Intell. Vehicles Symp., IEEE. (Sept. 2006) 238–243
10. Jaynes, C.O., Stolle, F., Collins, R.T.: Task driving perceptual organization for extraction of rooftop polygons. In: Appl. of Comp. Vis., Proc. IEEE Workshop on. (Dec. 1994) 152–159
11. Gates, J.W., Haseyama, M., Kitajima, H.: Real-time polygon extraction from complex images. In: Circuits and Systems, Proc. IEEE Int'l Symp. on. Volume 5. (May 2000) 309–312
12. Ferreira, A., Fonseca, M.J., Jorge, J.A.: Polygon detection from a set of lines. In: Encontro Portugues de Computacao Grafica. (Oct. 2003)
13. Croitoru, A., Doytsher, Y.: Right-angle rooftop polygon extraction in regularized urban areas: Cutting the corners. Photogrammetric Record, The 19(108) (Dec. 2004) 311–341
14. Zhu, Y., Carragher, B., Mouche, F., Potter, C.: Automatic particle detection through efficient Hough transforms. Medical Imaging, IEEE Trans. on 22(9) (Sept. 2003) 1053–1062

15. Shaw, D., Barnes, N.: Regular polygon detection as an interest point operator for SLAM. In: Australasian Conference on Robotics and Automation. (2004)
16. Lutton, E., Martinez, P.: A genetic algorithm for the detection of 2D geometric primitives in images. In: Pat. Rec., Int'l Conf. on. Volume 1. (1994) 526–528
17. Barnes, N., Loy, G., Shaw, D., Robles-Kelly, A.: Regular polygon detection. In: Comp. Vis. IEEE Int'l Conf. on. (2005)
18. Macieszczak, M., Ahmad, M.O.: Extraction of shape elements in low-level processing for image understanding systems. In: Elec. and Comp. Eng., Canadian Conf. on. Volume 2. (Sept. 1995) 1184–1187
19. Liu, L., Sclaroff, S.: Deformable shape detection and description via model-based region grouping. In: Comp. Vis and Pat. Rec., IEEE Conf. on. Volume 2. (June 1999)
20. Moon, H., Chellappa, R., Rosenfeld, A.: Optimal edge-based shape detection. Image Proc., IEEE Trans. on 11(11) (Nov. 2002) 1209–1227
21. Amit, Y., Geman, D., Fan, X.: A coarse-to-fine strategy for multi-class shape detection. Pat. Anal. and Mach. Intell., IEEE Trans on 28 (2004) 1606–1621
22. Gidney, M.S., Diduch, C.P., Doraiswami, R.: Real-time post determination of polygons in a 2-D image. In: Elec. and Comp. Eng., Canadian Conf. on. Volume 2. (1995) 913–915
23. Miller, J.V., Breen, D.E.,Wozny, M.J.: Extracting geometric models through constraint minimization. In: Visualization, IEEE Conf. on. (Oct. 1990) 74–82
24. Mayer, S.: Constrained optimization of building contours from high-resolution ortho-images. In: Image Proc., IEEE Int'l Conf. on. Volume 1. (Oct. 2001) 838–841
25. Wang, Z., Ben-Arie, J.: Detection and segmentation of generic shapes based on affine modeling of energy in Eigenspace. Image Proc, IEEE Trans on. 10(11) (Nov. 2001) 1621–1629
26. Felzenszwalb, P.: Representation and detection of deformable shapes. Pat. Anal. and Mach. Intell., IEEE Trans on 27(s) (Feb. 2005) 208–220
27. Kanatani, K.: Group Theoretical Methods in Image Understanding. Springer, New York (1990)
28. Pikaz, A., Dinstein, I.: Matching of partially occluded planar curves. Pat. Rec. 28(2) (Feb. 1995) 199–209
29. Sebastian, T., Klein, P., Kimia, B.: On aligning curves. Trans. Pat. Anal. and Mach. Intell. 25(1) (2003) 116–125
30. Harris, C., Stephens, M.: A combined corner and edge detector. In: Alvey Vision Conference, Proc. (1988) 147–151
31. Smith, S., Brady, J.: SUSAN - A new approach to low level image processing. Int'l J. Comp. Vis. 23(1) (May 1997) 45–78
32. Huttenlocher, D., Kladerman, G., Rucklidge, W.: Comparing images using the Hausdorff distance. Trans. Pat. Anal. and Mach. Intell. 15(9) (Sept. 1993) 850–863
33. CASIL: California Spatial Information Library. http://archive.casil.ucdavis.edu/casil/ Last visited 17 Nov. 2006.